JOURNAL OF GEOPHYSICAL RESEARCH, VOL. 106, NO. D23, PAGES 31,717–31,727, DECEMBER 16, 2001

Variations with elevation in the surface energy balance on the Pasterze (Austria)

Wouter Greuell

Institute for Marine and Atmospheric Research, Utrecht University, Utrecht, Netherlands

Paul Smeets

Faculty of Earth Sciences, Vrije Universiteit Amsterdam, Amsterdam, Netherlands

Abstract. This paper presents the surface energy balance at five locations on the Pasterze, a glacier in Austria, during a period of 46 days in the summer of 1994. The computations are based on local measurements of radiative fluxes, wind speed, atmospheric temperature and humidity, and precipitation. These measurements served as input for a numerical mass-balance model that computes the surface temperature by simulation of subsurface processes. The surface temperature was then used for the computation of the outgoing long-wave radiative flux and for the computation of the turbulent fluxes by means of the "bulk method." Values of the roughness length for momentum were computed by profile analysis. They ranged from 1.2 to 5.8 mm. At all locations, net short-wave radiation constituted the dominant energy flux, the latent heat flux was small, and the net long-wave radiative flux and the sensible heat flux were of intermediate magnitude. The energy balances at the three stations on the glacier tongue were similar to each other but differed from those at the two stations in the accumulation basin, which were also similar to each other. These similarities within the two areas are due mainly to the fact that during the experiment there was hardly any variation in temperature and albedo within the two areas. The ablation rate at U3 (2420 m above sea level (asl)) was even slightly higher than the ablation rate at A1 (2205 m asl). At all stations the calculated mass balance agrees within 5% with the measured mass balance, which is within the margins determined by the uncertainties in the input variables and the model parameters and equations. This gives some confidence in the method used to compute the turbulent fluxes, but on the other hand, the agreement may also be caused by cancellation of errors. Because of the high temperatures during PASTEX the calculated mass balance would have been almost identical if the "zero-degree assumption" had been used instead of the subsurface module.

1. Introduction

With the exception of surging glaciers, glaciers and ice sheets are sensitive indicators of climatic variations. Their volume varies in time in response to temporal variations in accumulation and ablation and to temporal variations in ice temperature, which cause changes in ice-mechanical properties. Midlatitude glaciers are generally temperate, which means that the subsurface temperature is at melting point except for the part near the surface, which will generally cool below 0°C during the winter. Therefore geometric fluctuations of midlatitude glaciers are not due to variations in ice temperature but only to variations in accumulation and ablation. Variations in accumulation and ablation may both be important. This was demonstrated by *Holmlund et al.* [1996], who analyzed mass-balance measurements of Storglaciaren (Sweden). He found that on this glacier, interannual variations in winter accumulation and summer ablation are of similar magnitude. Thus climatic variations have significant effects on both winter accumulation and summer ablation, which together induce fluctuations in glacier volume.

Paper number 2001JD900127.
0148-0227/01/2001JD900127$09.00

In this paper we address the relation between climate and ablation by studying the surface energy balance as determined from measurements obtained on the Pasterze, a glacier in Austria. During summer 1994, measurements relating to the surface energy balance were made simultaneously at five different elevations on this glacier. The experiment, called PASTEX, resulted in a data set unique in the sense that simultaneous energy-balance measurements at so many elevations on a midlatitude glacier have not yet been described in the literature (though this has been done for the Greenland ice sheet by *Oerlemans and Vugts* [1993], for Antarctica by *Bintanja and van den Broeke* [1995], and for Vatnajökull on Iceland by *Oerlemans et al.* [1999]). The aim of this paper is to present and compare the energy balances at the five PASTEX locations. This will provide insight into the elevational variations in the energy balance of the Pasterze.

Earlier, *van den Broeke* [1997b] analyzed the surface energy balance for three PASTEX locations (A1, U2, and U5). The analysis presented in this paper differs from the analysis by *van de Broeke* [1997b] in several aspects. We consider five instead of three stations. We model the subsurface so that its influence on the energy balance is taken into account, whereas Van den Broeke (1997b) used the "zero-degree assumption" [see *Greuell and Oerlemans*, 1986]. Furthermore, we add some other elements. We correct the measurements of global radiation to obtain the incoming radiation for the tilting surface. We compare calculated with measured mass balance, and we discuss the sensitivity of the results for uncertainties in the measurements and in model parameters and equations.

The surface energy balance has been the topic of numerous previous papers. Some of these are based mainly on analysis of field measurements [e.g., *Ambach*, 1985; *Greuell and Oerlemans*, 1989; *Hock and Holmgren*, 1996; *Wagnon et al.*, 1999], whereas other papers describe model simulations with confirmation by mass-balance measurements [e.g., *Braithwaite and Olesen*, 1990; *van de Wal*, 1996] and without confirmation by mass-balance measurements [*Hoinkes and Wendler*, 1968; *Greuell and Oerlemans*, 1986].

2. Experimental Setup

The Pasterze (47°06'N and 12°43'E) is Austria's largest glacier with a surface area of 19.8 km^2 and a length of 9.2 km (in 1969 according to *Rott* [1993]). Its general exposure is southeast. A map of the glacier is shown in Figure 1.

Five energy-balance stations were established along the center flow line of the glacier, two in the main accumulation basin of the glacier (U4 and U5) and three in the ablation area on the glacier tongue (A1, U2, and U3). On average, during 1980-1984 the equilibrium line was located at 2800 m asl [*Tintor*, 1991]. Table 1 gives the elevation and the distance along the flow line of the stations. Along the flow line, connecting the stations, the slope is relatively gentle in both the upper part of the glacier (~ 7°) and the tongue (~ 5°), whereas it is much steeper in the icefall between these two parts of the glacier (up to 28°). At U4 and U5 the surface was covered by snow during the entire experiment, whereas the surface at the stations on the tongue consisted of ice, with the exception of U3, where the surface was covered by snow until June 26-29.

The energy-balance and mass-balance calculations for the locations of the stations were made with a surface energy-balance model (see section 4) based on measurements of the following variables: incoming and reflected short-wave radiative fluxes, incoming long-wave radiative flux, temperature, wind speed and humidity at the "2 m," and the "0.5 m" levels and precipitation. Computed mass balance was compared with measured mass balance. Radiative fluxes were measured in a horizontal plane. Since the stations were visited at least once per week, we had good control over the orientation of the radiation sensors (tilt less than 1°). Because of the weather conditions during the experiment, deposition of rime on the sensors was rare. The temperature sensors were ventilated. All the input variables and the mass balance were measured at each of the five stations, with the exception of the incoming long-wave radiative flux, which was not measured at U3 and U4, and precipitation, which was measured only at A1.

Before the expedition, in April 1994, many sensors were calibrated in the laboratory and just before (June 1-5) and after (August 23 to September 5) the expedition, all the instruments used on the Pasterze were set up for comparative measurements. This was done in Cabauw, approximately 20 km southwest of Utrecht, Netherlands. KNMI (Royal Dutch Meteorological Institute) sensors were used as reference sensors to determine corrections for our sensors. On the basis of specifications given by the manufacturers and the laboratory and field calibrations, the accuracy of the short-wave radiation components is estimated to be better than 2%, of the long-wave incoming radiation to be 10 W/m^2 and of temperature, wind speed, and relative humidity to be 0.2°C, 0.2 m/s, and 2%, respectively.

The mentioned heights of the temperature, wind, and humidity sensors (50 and 200 cm) are nominal. Ninety percent of the measurements on the glacier were taken between 13 and 71 cm, and 146 and 221 cm. The height of the radiation sensors varied from 100 to 170 cm.

For the determination of the mass balance, five stakes about 10 m apart were erected within 50 m of each glacier mast. Snow-density profiles were measured regularly as long as the surface consisted of snow.

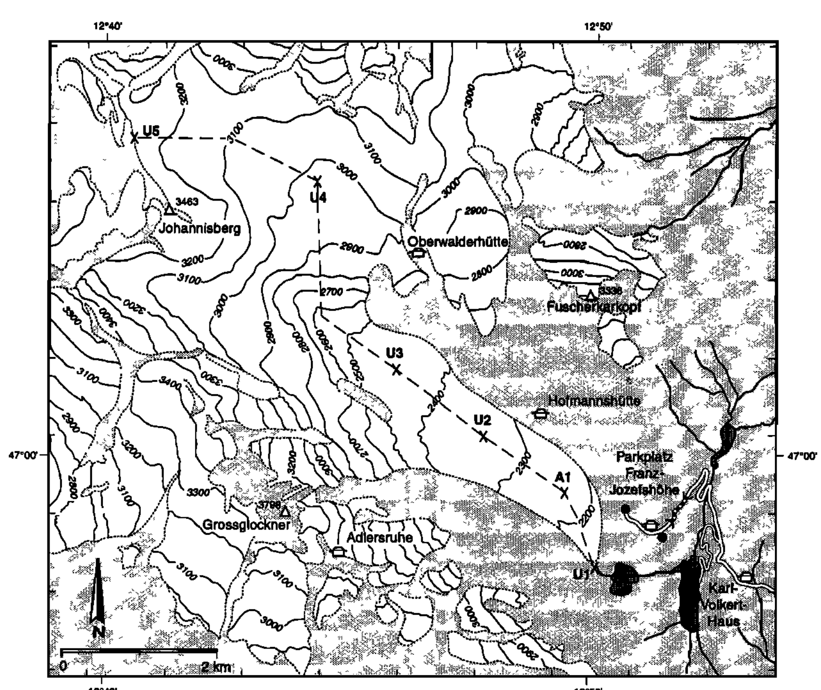

Figure 1. Map of the Pasterze. White surfaces are areas that were glaciated in 1985. The energy-balance stations discussed in this paper were located at A1, U2, U3, U4, and U5. The dashed line represents the "center flow line" mentioned in the paper.

Table 1. Elevation (in m asl) and Distance (in km) From the Ice Divide Along the Flow Line of the Energy-Balance Stations[a]

	A1 2205 m 7.9 km	U2 2310 m 6.6 km	U3 2420 m 5 2 km	U4 2945 m 2.3 km	U5 3225 m 0 1 km
Global radiation	252	267	273	301	283
Incoming short-wave radiation	256	272	278	307	286
Albedo	0.21	0.29	0.25	0.59	0.60
Net short-wave radiation	203	192	210	125	116
Incoming long-wave radiation	299	299	296	282	274
Outgoing long-wave radiation	315	315	315	314	313
Surface temperature (°C)	-0.1	-0.1	-0.1	-0.3	-0.7
Net long-wave radiation	-16	-16	-19	-32	-39
Directional constancy	0.94	0.96	0.97	0.81	0.07
Wind speed at 2 m (m/s)	4.1	4.5	4.6	4.3	4.4
Temperature at 2 m (°C)	6.8	6.4	7.1	3.5	3.2
z_0 (mm)	2.6	1.2	5.8	1.3	2.0
Sensible heat flux	48	53	63	23	20
Humidity mixing ratio at 2 m (g/kg)	5.5	5.5	5.5	5.7	5.5
Latent heat flux	10	11	10	5	1
Total energy flux	243	240	264	121	98
Measured net ablation rate (mm water equivalent/d)	61.3	63.1	66.9	32.1	24.0
Calculated - measured net ablation rate (mm water equivalent/d)	1.6	-1.4	1.6	1.7	0.8
Excess energy flux from atmosphere to glacier	+6	-5	+6	+7	+3

[a]Mean values of the components of the surface energy balance and of related variables between June 22, 0000 LT and August 7, 0000 LT. All quantities are given in W/m^2, unless specified otherwise. Global radiation (measured) is defined as the incoming short-wave radiative flux with respect to a horizontal surface, whereas row 2 gives the incoming short-wave radiative flux with respect to the local surface (computed). The last row gives the difference between calculated and measured ablation in terms of the equivalent energy flux.

More details about the types and accuracy of the instruments, gaps in the data sets, and the total periods of the measurements can be found in the works of *Greuell et al.* [1995, 1997] and *Obleitner and De Wolde* [1999]. In addition to the measurements mentioned above, other measurements, which are indirectly related to the surface energy balance but not used for the energy-balance calculations, were performed during PASTEX. Wind direction was measured at all of the five stations and the outgoing long-wave radiative flux at A1. Another energy-balance station (U1) was located on the end moraine only about 10 m away from the terminus. At A1 we performed measurements of temperature, wind speed, and humidity at six other levels in addition to the "2 m" and the "0.5 m" level, up to a height of 13 m. Also at this site, turbulent fluxes were measured directly by eddy correlation at 10 and 4 (or 2.5) m, and balloon soundings were made up to a height of 1000 m above the surface. The 13 m profile and the turbulence data from A1 were analyzed by *Smeets et al.* [1998, 2000], whereas *van den Broeke* [1997a, 1997b] used both the 13 m profiles and the balloon soundings to study the katabatic wind layer.

3. Variations With Elevation in Meteorological Variables

Variations in the energy balance with elevation are caused by variations in meteorological variables with elevation. Observations during PASTEX of the latter were treated in detail by *Greuell et al.* [1997] and *Greuell and Böhm* [1998], but since they are crucial for a proper understanding of the elevational variation in the energy balance, a summary is given here.

The measurements were, of course, affected by the mean meteorological conditions during PASTEX. Temperatures were relatively high. On Sonnblick (3106 m asl, 20 km east of the Pasterze) the mean summer temperature (JJA) in 1994 was 3.0°C. This is equal to the highest value during the period 1887-1989, whereas on average during the same period the mean summer temperature was 0.6°C [*Böhm*, 1992]. A typical daily course consisted of a morning with clear skies, followed by the appearance of clouds and occasional rain and thunderstorms during the afternoon.

Mean values of meteorological variables at the different stations for the period of the energy-balance calculations (June 22, 0000 LT - August 7, 0000 LT) are listed in Table 1.

Global radiation (= incoming short-wave radiative flux with respect to a horizontal surface) increased with elevation along most of the glacier, namely, from 252 W/m^2 at A1 to 301 W/m^2 at U4. Calculations show that under clear-sky conditions there is an increase in global radiation with elevation that can be ascribed to the general increase in surface albedo with elevation and to the fact that with increasing elevation a smaller fraction of the upper hemisphere is occupied by the surrounding mountains. Higher surface albedos lead to more incoming radiation due to multiple reflection between the surface and the atmosphere. Lower horizons also lead to more incoming radiation because of less horizon obstruction. Also, because of the general increase in albedo with elevation, energy gains caused by reflections from adjacent slopes tend to increase with elevation despite generally lower horizons. The mean effect of clouds is to enhance the elevational increase in global radiation between A1 and U4 prevailing during clear-sky conditions. However, between U4 and U5 the opposite is true; so on average, global radiation at U5 (283 W/m^2) is less than at U4 (301 W/m^2). Elevational variations in absolute optical path length and atmospheric water vapor and aerosol content explain only an insignificant part of the differences in the global radiation at the various stations.

Landsat data for July 30 show the variation in the surface albedo along the center flow line connecting the stations. The snow above the icefall had albedos between 0.54 and 0.60. The ice below the icefall had much lower albedos, namely, between 0.16 and 0.28. However, there was no systematic variation with elevation within these two areas. The variations in the daily values of the albedo during the experiment are plotted in Figure 2. On the glacier tongue (A1, U2, and U3) the albedos measured on 30 July were representative for the entire summer. At these stations the albedos did not show a trend during the experiment, with the exception of U3, where the surface was covered by snow during the first few days of the experiment. On the other hand, because of metamorphosis of the snow the albedos at U4 and U5 tended to decrease with time, interrupted by peaks caused by fresh snow.

Greuell et al. [1997] made a comparison of the incoming long-wave radiative fluxes at U2, located on the tongue (2310 m asl), and U5, located near the crest (3225 m asl). On average, this flux amounts to 299 W/m^2 at U2 and 274 W/m^2 at U5. Thus the station on the tongue receives 25 W/m^2 more than the station near the crest. Calculations indicate that this difference would have been almost twice as large (48 W/m^2) if clear-sky conditions had prevailed during the entire experiment. Most of the clear-sky difference between the two stations (39 W/m^2) is explained by the higher temperature and the higher humidity content of the atmosphere above U2 as compared to the atmosphere above U5. The remaining part of the clear-sky difference (9 W/m^2) is due to slopes, which occupy more of the upper hemisphere at U2 than at U5. The measured difference (25 W/m^2) between U2 and U5 is smaller than the calculated clear-sky difference (48 W/m^2). This suggests that the mean cloud amount is larger at U5 than at U2.

During PASTEX, glacier winds dominated the near-surface layer. At all stations, mean wind vectors pointed downward along the local slope. The directional constancy, defined as the ratio of the magnitude of the time-averaged wind vector and the time-averaged wind speed, was high, except at U5, located near the crest. Mean wind speed hardly varied with elevation and was around 4 m/s.

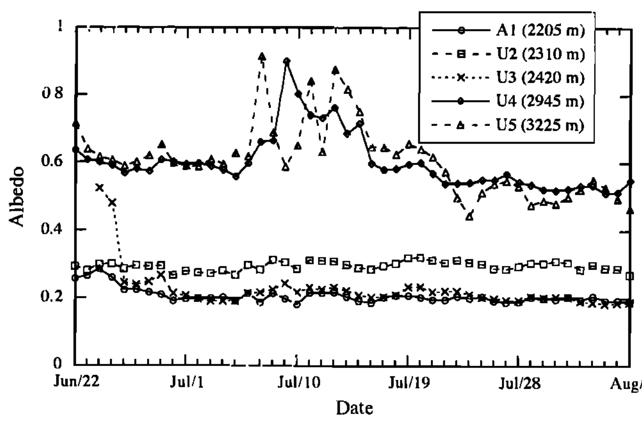

Figure 2. Ratio of daily means of outgoing and incoming short-wave radiative flux at the surface. The ground measurement at U2 for 30 July (0.30) lies outside the range of the albedo for the glacier tongue derived from the satellite data (0.16-0.28). This discrepancy is possibly due to subpixel variation in the albedo.

Particularly interesting is the distribution of the 2 m temperature along the glacier. As expected, temperatures over the tongue were higher (by about 3°-4°C) than over the accumulation basin. More surprisingly, 2 m temperatures at U4 and U5 were almost equal though the difference in elevation between these stations is 280 m, and there was even a reversal of the usual temperature gradient at the glacier tongue, where the temperature at U3 (2420 m asl) was 0.3°C higher than the temperature at A1 (2205 m asl). *Greuell and Böhm* [1998] explained this distribution by means of a simple thermodynamic glacier-wind model. This model assumes a glacier-wind layer with a thickness that is constant along the glacier. The temperature of parcels traveling down the glacier in this layer increases due to adiabatic heating and decreases due to turbulent exchange of sensible heat with the surface. In the limit of a horizontal surface, adiabatic heating vanishes, so parcels traveling "down" along the glacier only cool because of the sensible heat flux. The steeper the surface the more important the adiabatic heating becomes relative to cooling by the sensible heat flux. This explains the large increase in the 2 m temperature across the steep icefall and the fact that the temperature hardly changes with elevation in the accumulation basin and over the glacier tongue, where slopes are relatively gentle. Independent of the slope, cooling by the sensible heat flux is enhanced if ambient temperatures are high. Thus the model predicts that a "temperature reversal" over the glacier tongue occurs only when ambient temperatures are relatively high. This was the case during PASTEX.

The humidity mixing ratio was constant with elevation.

4. Energy-Balance Calculations

4.1. Energy-Balance Model

In this section we will discuss how the surface energy balance was computed from the available measurements. For this purpose we used the energy-balance model described in some detail by *Greuell and Konzelmann* [1994]. It consists of a part that computes the energy fluxes between the atmosphere and the glacier surface and a subsurface part. The model is forced by the following measured variables: incoming and outgoing short-wave radiation, incoming long-wave radiation, 2 m temperature, 2 m humidity, 2 m wind speed, and precipitation. Because of missing data, a generally small part of the input variables had to be found by interpolation or extrapolation in time or space. However, long-wave incoming radiation was not measured at all at U3 and U4. It was interpolated linearly with respect to elevation from the data at U2 and U5. Moreover, precipitation data were available only for A1. The amount of precipitation at the other locations was assumed to be the same. In the calculations, precipitation falls as snow, while 2 m temperatures are below 0°C, and as rain, while 2 m temperatures are above 0°C. The measurements of the incoming short-wave radiation were made with respect to a horizontal surface, i.e., as global radiation. Therefore a correction was applied for the magnitude and orientation of the slope to obtain the flux incident on the actual surface [see *Mannstein*, 1985]. Long-wave outgoing radiation was computed from the surface temperature on the assumption that the emissivity of snow and ice is equal to 1.0.

The surface temperature links the two parts of the model. It is needed both for the computation of the turbulent fluxes and for the computation of the outgoing long-wave radiative flux. It is calculated with the subsurface module. The subsurface module computes temperature, density, and water content on a one-dimensional grid extending approximately 25 m downward into the glacier. On this grid the following processes are described: formation, percolation, refreezing and runoff of meltwater, conduction, penetration of short-wave radiation, formation of slush and superimposed ice, and densification by compaction.

4.2. Computation of Turbulent Fluxes

A problem that merits special attention is the computation of the turbulent fluxes of sensible and latent heat. These fluxes could, in principle, be computed from the "2 m" and "0.5 m" values of the profile variables (wind speed, temperature, and humidity), using flux-profile relationships [e.g., *Stull*, 1988]. This method is generally referred to as the "profile method." The advantage of this method is that values of the usually unmeasured surface temperature and roughness lengths are not needed, but the disadvantage is that differences between the "2 m" and the "0.5 m" values of the profile variables tend to be small. More accurate values of the turbulent fluxes are generally obtained with the so-called "bulk method," which uses values of the profile variables at only one atmospheric level and at the surface. Contrasts between profile values at "2 m" and the surface are generally much larger than the contrasts between the "2 m" and the "0.5 m" values. Although surface values of the profile variables were not measured during PASTEX, they are fixed by theory (the wind speed at the ground is zero) or they can be calculated with good precision by means of the energy-balance model (temperature and humidity). The disadvantage of the "bulk method" is that the roughness lengths for momentum (z_o), temperature (z_T), and water vapor (z_q) must be known. These can be calculated from the profile variables at the "2 m" and the "0.5 m" level and the surface temperature, using a flux-profile relationship. This, again, introduces into the calculations the uncertainty in the differences between the profile variables at these two levels, suggesting that the "bulk method" suffers from the same problems as the "profile method." However, usually roughness lengths are not computed from all the individual profiles of wind speed, temperature, and humidity. Instead, a selection of near-neutral profiles is made. The advantage of these profiles is that buoyancy corrections in the flux-profile relationships are relatively small during near-neutral conditions, which makes estimates of z_o more accurate. The z_o values found for near-neutral conditions are then assumed to be valid for all conditions of stability because z_o is thought to be a function of the surface geometry only. Thereafter, values of z_T and z_q can be obtained from z_o and the wind profile (more precisely: the friction velocity) by means of the theory described by *Andreas* [1987] and confirmed by *Smeets et al.* [1998] and *Denby and Snellen* [2001] at A1.

During PASTEX the katabatic wind with wind maximums near the surface dominated. For instance, during 50% of the time, the highest wind speed at A1 was recorded at 4 m or lower. This makes the computation of the turbulent fluxes more complicated. The most widely used flux-profile relationships are those developed within the framework of the Monin-Obukhov similarity theory. A basic assumption in this theory is that fluxes are constant within the layer under consideration. Because of the low height of the wind maximum, however, this is not true in the layer up to a height of 2 m above the surface over midlatitude glaciers like the Pasterze [*Munro and Davies*, 1978; *Denby*, 1999]. Therefore one would expect the existing flux-profile relationships not to be valid within this layer. Nevertheless, *Denby and Greuell* [2000] compared turbulent fluxes computed with the "profile method" and the "bulk method" with the "real" surface fluxes at the surface. They did so with a second-order closure model for the simulation of the katabatic-wind layer. This model gives satisfactory simulations of the observed profiles of temperature, wind speed, and momentum and sensible heat flux, especially in the katabatic wind layer, which in this context is the relevant part of the atmosphere [*Denby*, 1999]. The comparison for cases with a low height of the wind maximum leads to the conclusion that "the profile methods severely underestimate turbulent fluxes. The bulk method, on the other hand, only slightly overestimates the turbulent heat flux in the entire region below the wind maximum." In conclusion, for a melting glacier the "bulk method" is preferable to the "profile method" because (1) in the "bulk method" the contrasts between the profile variables are larger and (2) model results support the "bulk method."

Therefore in this study the "bulk method" was employed. The surface values of the profile variables were combined with the "2 m" values of the profile variables and not with the "0.5 m" values. The disadvantage of the height of "0.5 m" is that uncertainties in the height of the sensors (surfaces were uneven with, at U3, bumps up to 0.5 m in height) have a relatively large effect on the calculated fluxes. On the other hand, at A1 the wind maximum was below the "2 m" level for 19% of the time.

We used the flux-profile relationships found by *Högström* [1988] for both the computation of the fluxes and the computation of z_o. The computation of z_o was done as follows [see also *Denby and Smeets*, 2000]:

1. Half-hourly mean profiles of wind speed and temperature (only "2 m" and "0.5 m" values) were used to solve the flux-profile relationships. This does not only result in values of the turbulent fluxes of momentum and sensible heat, which are not interesting at this stage, but also in a value of the Monin-Obukhov length (L_{ob}), which is a function of the fluxes.

2. Since L_{ob} is a measure of the stability, it is used to select "near-neutral profiles" ($L_{ob} > 50$ m).

3. The selected "near-neutral profiles" of wind speed are extrapolated downward to the level where the wind speed is equal to zero by means of the flux-profile relationships. The height of this level is, per definition, equal to z_0. For a discussion of the error sources associated with this method, the reader is referred to *Munro* [1989]. As can be seen in Figure 3, the number of selected profiles increases with elevation, corresponding to a higher frequency of "near-neutral conditions" at higher elevations, where contrasts between the "2 m" temperature and the temperature of the surface tend to be smaller. Temporal variations in z_0 cannot be clearly distinguished at any station. For A1 and U2 this is perhaps due to the small number of samples. The scatter is relatively high for the snow at U4 and U5. At U5 this is perhaps due to inhomogeneous fetch conditions (the station is near the glacier margin; see Figure 1) and large variability of the wind direction (see the directional constancy in Table 1). We do not have an explanation for the large amount of scatter at U4.

4. Computation of the mean $\log(z_0)$ for each station. Our value of z_0 for A1 (2.6 mm) differs from the values found for

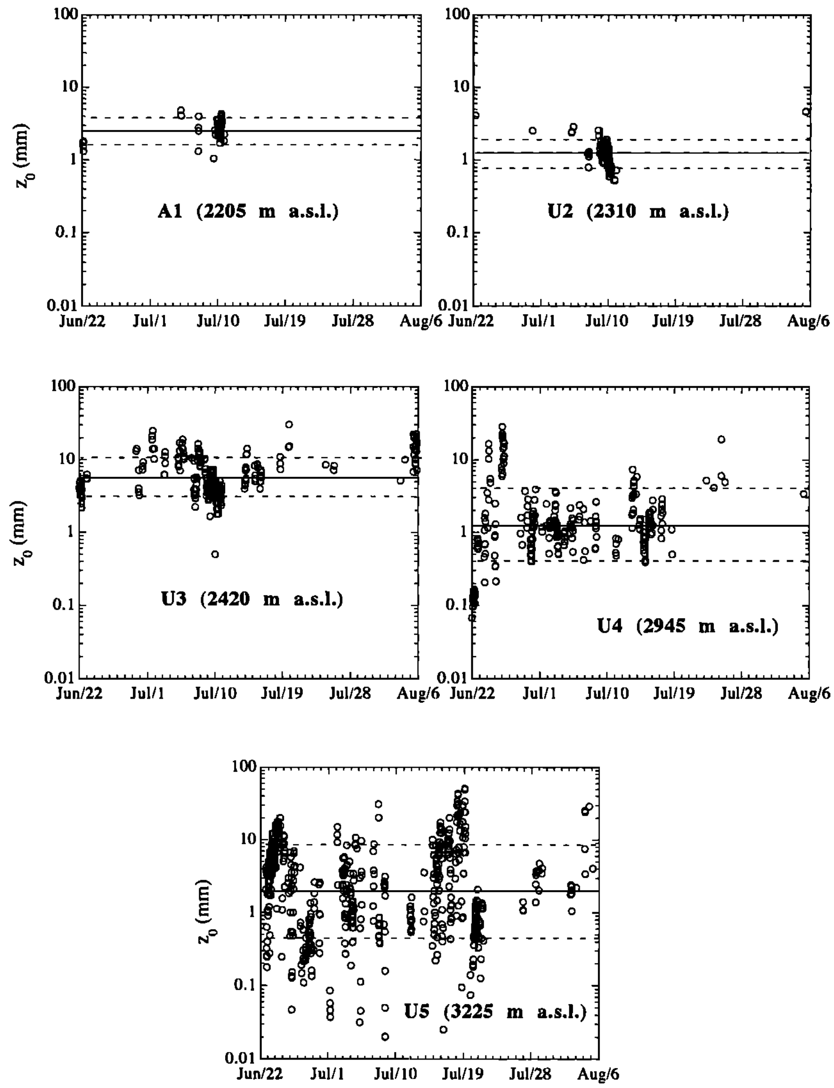

Figure 3. All values of the roughness length for momentum (z_0) determined from "near-neutral profiles." The continuous horizontal line and the broken horizontal lines correspond to the mean value and the standard deviation, respectively, for each station, where means and standard deviations were computed from log(z_0).

the same site by *van den Broeke* [1997b] (4.4 mm), *Smeets et al.* [1998] (1.0 mm), and *Denby and Smeets* [2000] (1.6 and 1.8 mm, dependent on the method). *Denby and Smeets* [2000] employed the same method as we used here to obtain the last value (1.8 m). However, they considered four measurement levels instead of two levels. The other values were obtained by different methods. A discussion of the reasons for the differences is beyond the scope of this paper. It is important to note, though, that the effect of using one of the other values of z_0 has a relatively small effect on the calculated mass balance (see section 5).

The mean value of z_0 for each station was used as input for the energy-balance computations. There is overlap of the values for the ice-covered glacier tongue (1.2 - 5.8 mm) with those for the snow-covered accumulation basin (1.3–2.0 mm). All these values are well within the range of values (0.9-11.0 mm) for snow and ice (excluding fresh snow), found at many different locations by analyzing profile measurements and listed by *Morris* [1989]. Our ice values are also similar to those for glacier ice listed by *Braithwaite* [1995], most of which are between 1 and 7 mm.

Values for the scalar roughness lengths z_T and z_q were calculated from z_0 and the friction velocity by means of the equations proposed by *Andreas* [1987]. On average for each station, z_T and z_q were 1-3 orders of magnitude smaller than z_0. It is noteworthy that the equations of Andreas predict a decrease in z_T and z_q with increasing z_0, which reduces the sensitivity of the sensible and latent heat flux to uncertainty in z_0.

4.3. Initialization

Initial temperature, density, and water-content profiles were taken as uniform with depth at all locations, except at U3, where the ice was overlaid with a snowpack of 35 cm water equivalent at the beginning of the experiment. The temperature was set equal to 0°C, the density of ice (A1, U2, and U3) equal to 910 kg/m^3, and the density of snow equal to the mean of the whole snowpack as measured at the start of the experiment. The initial water saturation was taken equal to the residual saturation (0.10 in the model). This means that 10% of the pore volume is filled by water.

5. Results

Figure 4 and Table 1 give the time-averaged values of the components of the surface energy balance. At all locations net short-wave radiation constitutes the dominant energy flux, the latent heat flux is small, and the net long-wave radiative flux and sensible heat flux are of intermediate magnitude. Because the subsurface temperature is at the melting point both at the beginning and at the end of the experiment, the sum of the radiative and the turbulent fluxes is used entirely for melting. Sensible heat deposited on the glacier by rain is negligible.

The mass balance and the energy balances at the three sites on the tongue are similar to each other; this applies also to the energy balances at the two sites in the accumulation basin. This is due to the fact that all the variables that determine the energy balance are more or less constant within these two areas. In this context the lack of variation in elevation of the atmospheric temperature and the albedo within the two areas is noteworthy. Usually, it is assumed that the temperature decreases with elevation, and it is often assumed that the albedo of glacier ice increases with elevation [e.g., *Oerlemans et al.*, 1991/1992]. Indeed, differences in atmospheric temperature and albedo are the main causes of the difference between the energy balances of the sites on the tongue and the energy balances of the sites in the accumulation basin. Variations in atmospheric temperature have an effect on both the turbulent flux of sensible heat and the incoming long-wave radiation, whereas variations in albedo determine the amount of absorbed solar radiation.

Measurements of the annual mass balance made on the tongue of the Pasterze [see *Tintor*, 1991] reveal the usual increase in mass balance with elevation. Possibly, the discrepancy between this fact and the absence of a mass-balance gradient during PASTEX (actually the ablation rate at U3 was higher than the ablation rate at A1, though A1 was located 215 m of elevation below U3) is caused by a combination of two factors. Firstly, the annual accumulation is expected to increase with elevation because precipitation probably increases with elevation as suggested by measurements carried out in northern Carinthia [*Auer et al.*, 1995] and because the fraction of precipitation falling as snow increases with elevation [*Rasmussen et al.*, 2000]. During PASTEX no snowfall occurred on the glacier tongue, so there was no accumulation gradient. Secondly, the small temperature variation on the glacier tongue during PASTEX probably differs from the mean temperature variation during the ablation season. As discussed in section 3, the temperature distribution is a function of the ambient temperature. Abnormally high ambient temperatures during PASTEX led to the "temperature reversal" between U3 and A1. The model of *Greuell and Böhm* [1998] suggests that the temperature would have decreased with elevation at a lower, more "normal" ambient temperature.

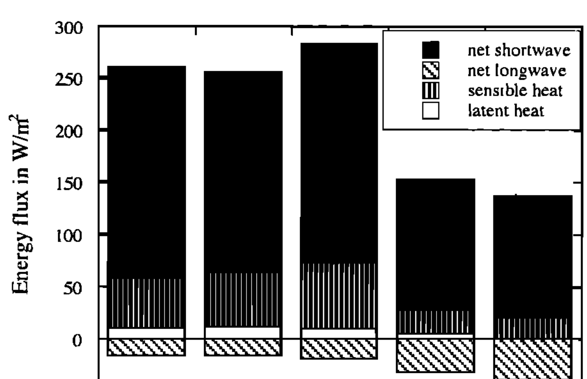

Figure 4. Mean values of the components of the surface energy balance on the Pasterze between June 22, 0000 LT, and August 7, 0000 LT, 1994. Differences between stations are to a large extent due to differences in albedo (α) and 2 m air temperature (T).

Figure 5 shows the mean daily cycles of the components of the energy balance for the 46-day period of the energy-balance calculations. Daily cycles of temperature, wind speed, and humidity are also depicted to facilitate the interpretation of the daily cycles of the energy-balance components. Only U2 and U5 are considered. Daily cycles at A1 and U3 were similar to those at U2, whereas daily cycles at U4 were similar to those at U5.

The daily variation in the net long-wave radiative flux is dominated by the daily variation in the incident flux. If the sky had been clear all the time, the variation in the incident flux would have been caused mainly by variations in atmospheric temperature (observed range at 2 m of ~ 3°C) and hardly by variations in atmospheric water vapor pressure (observed range at 2 m of 60-140 Pa). This follows from calculations with a parameterization for the incoming long-wave radiative flux presented by *Greuell et al.* [1997, equation (5)]. Nevertheless, maximums (19-20 hours) and minimums (8-10 hours) in the incoming long-wave radiative flux occur some hours later than the maximums (15-17 hours) and minimums (2-6 hours) in the 2 m air temperature but coincide approximately with the less well-defined maximums (20-21 hours at U2 and 16-19 hours at U5) and minimums (8-11 hours) in 2 m vapor pressure. This discrepancy can perhaps be explained by clouds, which probably have a daily cycle in amount and/or optical thickness in phase with atmospheric humidity. In other words, maximums and minimums in the daily cycle of cloud amount and/or optical thickness coincide with maximums and minimums in the daily cycle of atmospheric humidity and cause maximums and minimums in the daily cycle of the incoming long-wave radiative flux.

In the first place the daily variation in the sensible heat flux at U2 can be ascribed to the daily variation in atmospheric temperature. All other things being equal, higher 2 m temperatures are caused by higher temperatures of the free atmosphere and therefore correspond to larger temperature deficits over the melting surface. This affects the katabatic wind, which is forced by the temperature deficit. Higher temperature deficits, corresponding to higher air temperatures, generate stronger winds. This explains why at U2 the wind speed is in phase with the air temperature. Because at U2 the daily variation in the surface temperature is negligible, variations in atmospheric temperature and wind speed explain almost the entire variation in the sensible heat. At U5 this is not true because at that location the surface cools by approximately 2°C during the night. This

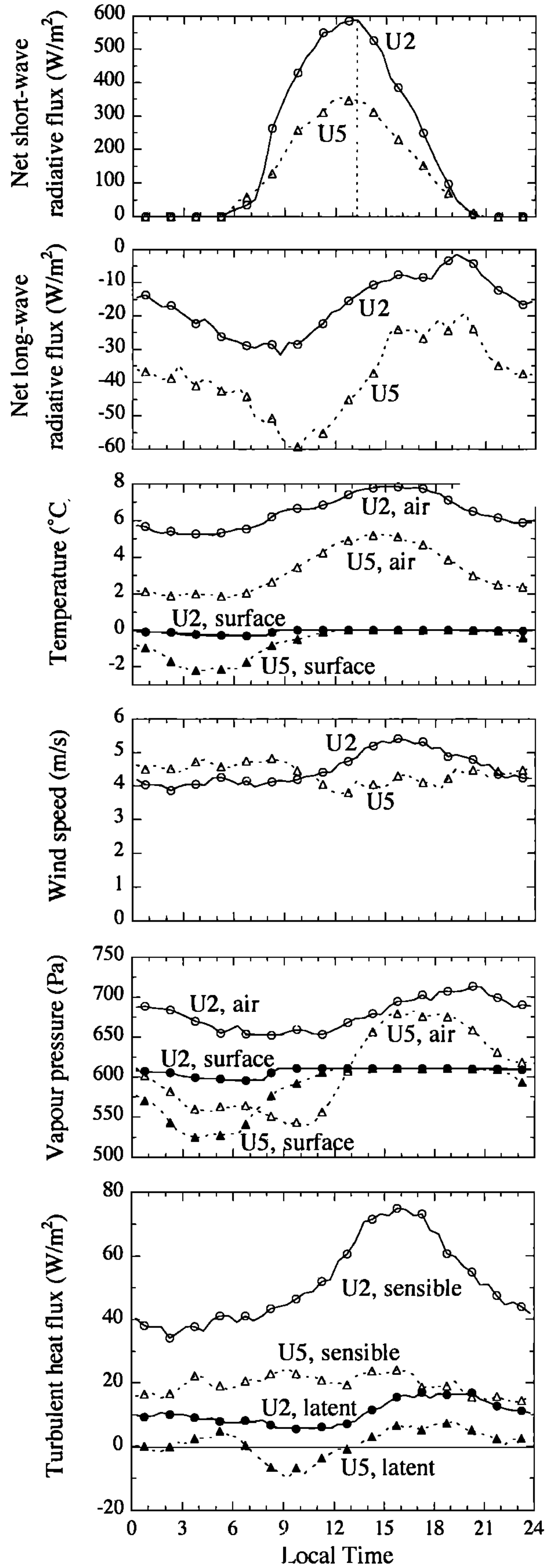

Figure 5. Mean daily cycles of the components of the surface energy balance and of some profile variables between June 22, 0000 LT, and August 7, 0000 LT, 1994. Results are shown for U2 (2310 m asl) and U5 (3225 m asl). The dashed line in the topmost panel corresponds to local solar noon.

cooling enhances the temperature contrast between atmosphere and surface during the night, which is consequently only slightly smaller than in daytime. Because of the combination of this daily cycle in temperature contrast with the daily variation in wind speed (maximum during the late night) the daily variation in sensible heat flux is small at U5.

Both at U2 and U5 there is a clear daily cycle in the latent heat flux. The maximums and minimums of the daily cycle coincide with maximums and minimums in atmospheric vapor pressure, which in turn are linked to the mountain-valley-wind system according to *van den Broeke* [1997b].

All our calculations were made without any tuning. As a result there are differences between calculated and measured net ablation (Table 1). For the five stations these differences range from −1.4 to 1.7 mm water equivalent/d, on average, over the entire 46-day period. In terms of energy fluxes the difference does not exceed 7 W/m^2, which seems a small discrepancy in view of the total energy fluxes between atmosphere and glacier (Table 1). Nevertheless, the question is whether the differences are acceptable in view of the known uncertainties affecting calculated and measured mass balance, namely, uncertainties in the input variables, in the model parameters, in the equations, and in the measured mass balance. The effect of the uncertainty in the input variables was determined by performing sensitivity runs. In each sensitivity run, one of the input variables was increased or decreased relative to the standard run by an amount equal to the assumed uncertainty. Then, for each variable the resulting absolute values of the changes in the computed ablation rate were averaged over the 10 runs (5 stations times 2 runs). Similar sensitivity runs were performed to determine the uncertainty in the calculations due to the uncertainty in z_0, given by the standard deviation of the individual z_0 values plotted in Figure 3. We also tested the effect of using different formulations for the flux-profile relationships, namely, those proposed by *Businger et al.* [1971], those proposed by *Dyer* [1974], and those proposed by *Beljaars and Holtslag* [1991]. The latter gave the best fit to measurements performed over the Greenland ice sheet by *Forrer and Rotach* [1997].

Table 2 lists the uncertainties in the calculated net ablation due to the uncertainties in the input variables, in z_0 and the flux-profile relationships. The total uncertainty in the calculations (the square root of the sum of the squares of the individual uncertainties: 3.6 mm water equivalent/d) is caused largely by the uncertainties in the incoming fluxes of short-wave and long-wave radiation. Among the different formulations for the flux-profile relationships, replacement of the relationships of *Högström* [1988] by those of *Dyer* [1974] resulted in the largest absolute difference in calculated mass balance (0.7 mm water equivalent/d). There is also uncertainty in the measured mass balance (1.5 mm water equivalent/d). This value was found by computing for each station the standard deviation of the ablation measured along the five stakes and, subsequently, taking the mean of the standard deviations found for the different stations. In view of these estimates of the uncertainties in the calculated and measured net ablation, the differences between calculations and measurements are acceptable.

6. Conclusions and Discussion

This paper presents the surface energy balance at five locations on the Pasterze, a glacier in Austria, during a period of 46 days in the summer of 1994. At all locations, net short-wave

Table 2. Effect on Calculated Ablation of Small Changes in a Number of Input Variables in the Roughness Length for Momentum and of Using Different Formulations for the Flux-Profile Relationships[a]

Measured Variable / Model Parameter	Uncertainty	Resulting Uncertainty in Computed Net Ablation (mm water equivalent/d)
Incoming short-wave radiative flux	2%	1.9
Reflected short-wave radiative flux	2%	0.8
Incoming long-wave radiative flux	10 W/m^2	2.4
Temperature	0.2°C	0.9
Wind speed	0.2 m/s	0.8
Relative humidity	2 %	0.8
Momentum roughness length	see Figure 3	0.8
Flux-profile relationships	*Businger et al* [1971]	0 0
	Dyer [1974]	0.7
	Beljaars and Holtslag [1991]	0.3
Total effect on calculations		3.6

[a]Changes in the input variables and in z_0 were chosen equal to the uncertainties in these variables.

radiation constitutes the dominant energy flux, the latent heat flux is small, and the net long-wave radiative flux and the sensible heat flux are of intermediate magnitude. The energy balances of the stations on the glacier tongue are similar to each other, as are the energy balances of the stations in the accumulation basin. These similarities are due mainly to the fact that both temperature and albedo hardly vary within these two areas.

The derived energy balances are based on local measurements of radiative fluxes, wind speed, atmospheric temperature and humidity, and precipitation. The "bulk method" was used for the computation of the turbulent fluxes. We discussed in some detail why this method is preferable to the "profile method." The "bulk method" can be applied only if the surface temperature and the roughness lengths are known. The surface temperature was computed by means of a numerical model that simulates subsurface processes. The roughness length for momentum was computed by profile analysis, and the theory of *Andreas* [1987] was used for the computation of the scalar roughness lengths.

At all stations the calculated mass balance agrees with the measured mass balance within the uncertainty margins determined by the uncertainties in the input variables and the model parameters and equations. This suggests that real values of the input variables and model parameters (notably the roughness lengths) are within the assumed uncertainty margins and, more importantly, that the method used to compute the turbulent fluxes is indeed correct. It should be realized, however, that the five determinations of calculated minus measured mass balance are not independent. If the incoming radiative fluxes are too high at one site, they are probably too high at all sites because calibration of the instruments is not independent. The same is true for the turbulent fluxes because the method employed to compute these fluxes is identical at all sites. Therefore if there is agreement between calculated and measured mass balance at one site due to cancellation of errors, the likelihood of agreement at the other sites increases. In conclusion, the results of the comparison give some confidence in the accuracy of the measurements and the appropriateness of the computational methods, but we cannot exclude that the agreement between calculated and measured mass balance is caused by cancellation of errors.

It should be noted that substitution of the subsurface part of the model by a "zero-degree assumption" would have given almost the same results. The difference between net ablation calculated with our subsurface module and net ablation calculated with the "zero-degree assumption" does not exceed 0.5 mm water equivalent/d at all of the stations, except at U4 where computed net ablation increases by 2.4 mm water equivalent/d, using the "zero-degree assumption" instead of the subsurface module. Indeed, according to the calculations with the full model, the mean surface temperature did not differ much from 0°C at all of the stations (see Table 1). This is mainly due to the atmospheric temperatures, which were particularly high during PASTEX. At lower atmospheric temperatures the "zero-degree assumption" would have failed [*Greuell and Oerlemans*, 1986].

Finally, the role of the microtopography and of spatial inhomogeneities in the albedo around the stakes and the meteorological masts may have caused biases in the measured and the calculated mass balance. This is probably of less importance in the snow-covered area (U4 and U5), but it may not be negligible in the ice-covered area (A1, U2, and U3). The ice generally showed more relief than the snow. Bumps typically had a horizontal dimension of 5-10 m. During the experiment they became especially high (up to approximately 0.5 m) at U3.

Near-surface profiles of wind speed, temperature, and humidity above bumps will be different from the profiles above the gullies. Therefore turbulent fluxes derived from either of these sets of profiles will be different, but currently it is not possible to make an estimate of the magnitude of the difference. Specifically designed experiments are needed to do this. In any case, since our masts were generally located on bumps, the turbulent fluxes derived from our profile data may not be representative of the mean turbulent fluxes for an area with dimensions equal to several times the typical dimension of the bumps.

Bumps and gullies also have different albedos. Morainic material tends to accumulate in the gullies, which consequently have lower albedos than the bumps (estimated order of magnitude of the difference is 0.10, but the difference depends on the scale). During PASTEX, sensors typically "saw" an area with a radius of only 5 m, and masts in the ablation area were generally located on bumps. Hence the measured albedos are biased toward the higher values of the bumps.

Stakes sometimes "moved into" gullies, but generally they were located on bumps. Therefore the computed turbulent fluxes, the measured albedos, and the measured mass balances are probably all biased toward the bumps. It should be realized that if this had not been the case, differences between calculated and measured mass balance would have been much larger. For instance, a change of 0.10 in albedo causes a change in ablation of approximately 4 mm water equivalent/d (see Table 2), which is significant compared to the mean differences between calculated and measured ablation (ranging between -1.4 and 1.7 mm water equivalent/d; see Table 1).

Acknowledgments. We are very grateful to all the people involved in the field work, to Bruce Denby for his calculations of the momentum roughness length, to members of the Ice and Climate Group of the IMAU, whose comments helped us to improve this paper, and to Sheila McNab, who improved the English. The Pasterze project was financed by the Commission of the European Communities (contract EV5V-CT91-0051), the Dutch National Research Programme on Global Air Pollution and Climate Change (contract 276/91-NOP), and the Netherlands Organisation for Scientific Research (NWO/GOA, contract 750.294.04B).

References

Ambach, W., Characteristics of the heat balance of the Greenland ice sheet for modelling, *J. Glaciol.*, *31*, 3-12, 1985.

Andreas, E. L., A theory for the scalar roughness and the scalar transfer coefficients over snow and sea ice, *Boundary Layer Meteorol.*, *38*, 159-184, 1987.

Auer, I., R. Böhm, N. Hammer, W. Schöner, T. Wiesinger, and W. Winiwarter, Glaziologische Untersuchungen im Sonnblickgebiet: Forschungsprogramm Wurtenkees, *Oester. Beitr Meteorol. Geophys.*, *12*, Zentralanst. für Meteorol. und Geodyn., Vienna, Austria, 1995.

Beljaars, A., and A. Holtslag, Flux parameterization over land surfaces for atmospheric models, *J. Appl. Meteorol.*, *30*, 327-341, 1991.

Bintanja, R., and M. R. van den Broeke, The surface energy balance of Antarctic snow and blue ice, *J. Appl. Meteorol.*, *34*(4), 902-926, 1995.

Böhm, R., Lufttemperaturschwankungen in Österreich seit 1775, *Publ. 341*, Zentralanst. für Meteorol. und Geodyn., Wien, Austria, 1992.

Braithwaite, R.J., Aerodynamic stability and turbulent sensible-heat flux over a melting ice surface, the Greenland ice sheet, *J. Glaciol.*, *41*, 562-571, 1995.

Braithwaite, R.J., and O.B. Olesen, A simple energy-balance model to calculate ice ablation at the margin of the Greenland ice sheet, *J. Glaciol.*, *36*, 222-228, 1990.

Businger, J.A., J.C. Wyngaard, Y. Izumi, and E.F. Bradley, Flux profile relationships in the atmospheric surface layer, *J. Atmos. Sci.*, *28*, 181-189, 1971.

Denby, B., Second order modelling of turbulence in katabatic flows, *Boundary Layer Meteorol.*, *92*(1), 67-100, 1999.

Denby, B., and W. Greuell, The use of bulk and profile methods for determining surface heat fluxes in the presence of glacier winds, *J. Glaciol.*, 46(154), 445-452, 2000.

Denby, B., and P. Smeets, Derivation of turbulent fluxes profiles and roughness lengths from katabatic flow dynamics, *J. Appl. Meteorol.*, *39*(9), 1601-1612, 2000.

Denby, B. and H. Snellen, Observed roughness lengths for momentum and temperature on a melting glacier surface, *Boundary Layer Meteorol.*, in press, 2001.

Dyer, A.J., A review of flux-profile relationships, *Boundary Layer Meteorol.*, *7*, 363-372, 1974.

Forrer, J., and M.W. Rotach, On the turbulence structure in the stable boundary layer over the Greenland ice sheet, *Boundary Layer Meteorol.*, *85*, 111-136, 1997.

Greuell, W., and R. Böhm, Two-metre temperatures along melting mid-latitude glaciers and implications for the sensitivity of the mass balance to variations in temperature, *J. Glaciol.*, *44*(146), 9-20, 1998.

Greuell, W., and T. Konzelmann, Numerical modelling of the energy balance and the englacial temperature of the Greenland Ice Sheet, Calculation for the ETH-Camp location (West Greenland, 1155 m asl), *Global Planet. Change*, *9*, 91-114, 1994.

Greuell, W., and J. Oerlemans, Sensitivity studies with a mass balance model including temperature profile calculations inside the glacier, *Z. Gletscherkd. Glazialgeol.*, *22*(2), 101-124, 1986.

Greuell, W., and J. Oerlemans, Energy balance calculations on and near Hintereisferner (Austria) and an estimate of the effect of greenhouse warming on ablation, in *Proceedings of the Symposium on Glacier Fluctuations and Climatic Change*, pp. 305-323, *Kluwer Acad., Norwell, Mass.*, 1989.

Greuell, W., M. van den Broeke, W. Knap, C. Reijmer, P. Smeets, and I. Struijk, PASTEX: A glacio-meteorological experiment on the Pasterze (Austria), internal report, Inst. for Mar. and Atmos. Res., Utrecht Univ., Utrecht, Fac. of Earth Sci., Vrije Univ. Amsterdam, Amsterdam, Netherlands, 1995.

Greuell, W., W.H. Knap, and P.C. Smeets, Elevational changes in meteorological variables along a midlatitude glacier during summer, *J. Geophys. Res.*, *102*, 25,941-25,954, 1997.

Hock, R., and B. Holmgren, Some aspects of energy balance and ablation of Storglaciären, northern Sweden, *Geogr. Ann.*, Ser.A, *78* (2-3), 121-132, 1996.

Högström, U., Non-dimensional wind and temperature profiles in the atmospheric surface layer: A re-evaluation, *Boundary Layer Meteorol.*, *42*, 55-78, 1988.

Hoinkes, H., and G. Wendler, Der Anteil der Strahlung an der Ablation von Hintereis- und Kesselwandferner (Ötztaler Alpen, Tirol) im Sommer 1958, *Arch. Meteorol. Geophys. Bioklim.*, *B*(16), 195-236, 1968.

Holmlund, P., W. Karlén, and H. Grudd, Fifty years of mass balance and glacier front observations at the Tarfala Research Station. *Geogr. Ann., Ser. A*, *78*, 105-114, 1996.

Mannstein, H., The interpretation of albedo measurements on a snow-covered slope, *Arch. Meteorol. Geophys. Bioklim., Ser. B*, *36*, 73-81, 1985.

Morris, E.M., Turbulent transfer over snow and ice, *J. Hydrol.*, *105*, 205-223, 1989.

Munro, D.S., Surface roughness and bulk heat transfer on a glacier: Comparison with eddy correlation, *J. Glaciol.*, *35*(121), 343-348, 1989.

Munro, D.S., and J.A. Davies, On fitting the log-linear model to wind speed and temperature profiles over a melting glacier, *Boundary Layer Meteorol.*, *15*, 423-437, 1978.

Obleitner, F., and J. de Wolde, On intercomparison of instruments used within the Vatnajökull glacio-meteorological experiment, *Boundary Layer Meteorol.*, *92*(1), 27-37, 1999.

Oerlemans, J., R.S. van de Wal, and L.A. Conrads, A model for the surface balance of ice masses, part II, Application to the Greenland ice sheet, *Z. Gletscherkd. Glazialgeol.*, *27/28*, 85-96, 1991/1992.

Oerlemans, J., and H.F. Vugts, A meteorological experiment in the melting zone of the Greenland Ice Sheet, *Bull. Am. Meteorol. Soc.*, *74*(3), 355-365, 1993.

Oerlemans J., H. Björnsson, M. Kuhn, F. Obleitner, F. Palsson, C.J.P.P. Smeets, H. F. Vugts, and J. de Wolde, Glacio-meteorological investigations on Vatnajökull, Iceland, summer 1996: An overview, *Boundary Layer Meteorol.*, *92*(1), 3-26, 1999.

Rasmussen, L.A., H. Conway, and P.S. Hayes, The accumulation regime of Blue Glacier, U.S.A., 1914-96, *J. Glaciol.*, *46*(153), 326-334, 2000.

Rott, H., The Austrian Alps, in *Satellite Image Atlas of Glaciers of the World*, part E, Europe, edited by R.S. Williams, and J.G. Ferrigno, U.S. Govt. Print. Off., Washington, D. C., 1993.

Smeets, C.J.P.P., P.G. Duynkerke, and H.F. Vugts, Turbulence characteristics of the stable boundary layer over a mid-latitude glacier, part I, A combination of katabatic and large-scale forcing, *Boundary Layer Meteorol.*, *87*, 117-145, 1998.

Smeets, C.J.P.P., P.G. Duynkerke, and H.F. Vugts, Turbulence characteristics of the stable boundary layer over a mid-latitude glacier, part II, Pure katabatic forcing conditions, *Boundary Layer Meteorol.*, *97*, 73-103, 2000.

Stull, R.B., *An Introduction to Boundary Layer Meteorology*, 666 pp., Kluwer Acad., Norwell, Mass., 1988.

Tintor, W., 10 Jahre Ablationsmesssungen an der Pasterze, *Carinthia 2*, 181./101., 277-299, 1991.

van den Broeke, M.R., Momentum, heat and moisture budgets of the katabatic wind layer over a midlatitude glacier in summer, *J. Appl. Meteorol.*, *36*(6), 763-774, 1997a.

van den Broeke, M.R., Structure and diurnal variation of the atmospheric boundary layer over a mid-latitude glacier in summer, *Boundary Layer Meteorol.*, *83*, 183-205, 1997b.

van de Wal., R.S.W., Mass-balance modelling of the Greenland ice sheet: A comparison of energy-balance and a degree-day model, *Ann. Glaciol.*, *23*, 36-45, 1996.

Wagnon, P., P. Ribstein, B. Francou and B. Pouyaud, Annual cycle of energy balance of Zongo Glacier, Cordillera Real, Bolivia, *J. Geophys. Res.*, *104*, 3907-3923, 1999.

W. Greuell, Institute for Marine and Atmospheric Research, Utrecht University, Princetonplein 5, NL 3584 CC Utrecht, The Netherlands. (w.greuell@phys.uu.nl)

P. Smeets, Faculty of Earth Sciences, Vrije Universiteit Amsterdam, De Boelelaan 1085, NL 1081 HV Amsterdam, The Netherlands.

(Received September 18, 2000; revised January 17, 2001; accepted January 29, 2001.)